Journal of Orthopaedic Translation 37 (2022) 37–45

Contents lists available at ScienceDirect

Journal of Orthopaedic Translation

journal homepage: www.journals.elsevier.com/journal-of-orthopaedic-translation

Original article

Irisin promotes fracture healing by improving osteogenesis and angiogenesis

Tianyou Kan [a,1], Zihao He [a,b,1], Jingke Du [a,c,1], Mingming Xu [a], Junqi Cui [d], Xuequan Han [a,e], Dake Tong [a], Hanjun Li [f], Mengning Yan [a], Zhifeng Yu [a,*]

[a] Shanghai Key Laboratory of Orthopedic Implants, Department of Orthopedic Surgery, Shanghai Ninth People's Hospital, Shanghai Jiao Tong University School of Medicine, Shanghai, China
[b] Arthritis Clinic & Research Center, Peking University People's Hospital, Beijing, China
[c] Institute of Sports Medicine, Peking University Third Hospital, Beijing, China
[d] Department of Pathology, Shanghai Ninth People's Hospital, Shanghai Jiao Tong University School of Medicine, Shanghai, China
[e] Department of Orthopaedics, Qilu Hospital, Shandong University Centre for Orthopaedics, Cheeloo College of Medicine, Shandong University, Jinan, Shandong, China
[f] Clinical Stem Cell Research Center, Ren Ji Hospital, Shanghai Jiao Tong University School of Medicine, Shanghai, China

ARTICLE INFO

Keywords:
Fracture healing
Myokine
Irisin
Osteogenesis
Angiogenesis

ABSTRACT

Background: Osteogenesis and angiogenesis are important for bone fracture healing. Irisin is a muscle-derived monokine that is associated with bone formation.

Methods: To demonstrate the effect of irisin on bone fracture healing, closed mid-diaphyseal femur fractures were produced in 8-week-old C57BL/6 mice. Irisin was administrated intraperitoneally every other day after surgery, fracture healing was assessed by using X-rays. Bone morphometry of the fracture callus were assessed by using micro-computed tomography. Femurs of mice from each group were assessed by the three-point bending testing. Effect of irisin on osteogenic differentiation in mesenchymal stem cells *in vitro* was evaluated by quantitative real-time polymerase chain reaction (qRT-PCR), alkaline phosphatase staining and alizarin red staining. Angiogenesis of human umbilical vein endothelial cells (HUVECs) were evaluated by qRT-PCR, migration tests, and tube formation assays.

Results: Increased callus formation, mineralization and tougher fracture healing were observed in the irisin-treated group than in the control group, indicating the better fracture callus healing due to Irisin treatment. The vessel surface and vessel volume fraction of the callus also increased in the irisin-treated group. The expression of BMP2, CD31, and VEGF in callus were enhanced in the irisin-treated group. In mouse bone mesenchymal stem cells, irisin promoted ALP expression and mineralization, and increased the expression of osteogenic genes, including *OSX*, *Runx2*, *OPG*, *ALP*, *OCN* and *BMP2*. Irisin also promoted HUVEC migration and tube formation. Expression of angiogenic genes, including *ANGPT1*, *ANGPT2*, *VEGFb*, *CD31*, *FGF2*, and *PDGFRB* in HUVECs were increased by irisin.

Conclusion: All the results indicate irisin can promote fracture healing through osteogenesis and angiogenesis. These findings help in the understanding of muscle–bone interactions during fracture healing.

The Translational Potential of this Article: Irisin was one of the most important monokine secreted by skeletal muscle. Studies have found that irisin have anabolic effect one bone remodeling through affecting osteocyte and osteoblast. Based on our study, irisin could promote bone fracture healing by increasing bone mass and vascularization, which provide a potential usage of irisin to promote fracture healing and improve clinical outcomes.

Abbreviations: BMP2, bone morphogenetic protein 2; CD31, platelet endothelial cell adhesion molecule-1; VEGF, vascular endothelial growth factor; ALP, alkaline phosphatase; OSX, osterix; Runx2, core-binding factor, alpha 3 subunit; OPG, osteoprotegerin; OCN, osteocalcin; HUVEC, human umbilical vein endothelial cells; ANGPT1, angiopoietin 1; ANGPT2, angiopoietin 2; VEGFb, vascular endothelial growth factor b; FGF2, fibroblast growth factor 2; PDGFRB, platelet-derived growth factor receptor b.

* Corresponding author.
E-mail address: zfyu@outlook.com (Z. Yu).

[1] These authors contributed equally to this study.

https://doi.org/10.1016/j.jot.2022.07.006
Received 9 January 2022; Received in revised form 27 June 2022; Accepted 15 July 2022

1. Introduction

Fractures and the bone repair process impose a huge burden on patients and society. Approximately, 5%–10% of fractures are subject to delayed healing or result in a non-union [1]. Non-union occurs when underlying pathologies lead to either the fracture callus failing to fully ossify, in atrophic cases, or not form altogether. Fracture healing is a complex procedure that involves the coordination of many different processes [2], among which angiogenesis and osteogenesis play very important roles [3,4]. Many tissues and cells are involved in these processes, including the bone marrow, periosteum, and vascular endothelium. During the fracture healing, cells and cytokines are transported to the fracture site through blood vessels (T. [5], and mesenchymal stem cells differentiate into chondrocytes and osteoblasts. Soft callus (cartilage) is formed, followed by the hard callus (bone) (T [5].

Muscle is the major soft tissue surrounding the bone. Fracture healing complication rates are much higher in fractures with muscle damage [6]. Vascularization plays an important role in the early stage of fracture healing, and the soft tissues surrounding the fracture site are an important source of blood vessels required for transporting oxygen, nutrients, and bone progenitor cells to the injured area [7]. In addition, the muscle can induce bone formation. In the fracture healing process, newly formed callus tissue tends to be the largest and most dense at the bone-muscle interface, indicating that the muscle contributes to the formation of the callus or provides a suitable biomechanical environment for its development [8]. In recent years, the muscle secretome (myokines) has increasingly garnered attention because of its important role in muscle–bone interactions.

Through the bone-muscle crosstalk, exercise can have many physical benefits largely owing to its association with angiogenesis, including a reduced muscle loss and a reduced risk of fractures. Physical exercise is recommended by the WHO as a prophylactic measure and treatment for osteoporosis [9]. Myokines, such as aminobutyric acids, can be used as biomarkers to evaluate the risk of osteoporosis fracture (Z [10]. Irisin is a muscle-derived monokine that is secreted in response to exercise. Irisin is a cleaved version of its precursor, fibronectin type III domain-containing 5 (FNDC5) protein [11]. Irisin was initially found to drive the conversion of white adipose tissue to brown adipose tissue [12]. Subsequently, the role of irisin in the skeletal system has gained attention, and Colaianni et al. have found that irisin affects bone formation (G [13,14]. Moreover, irisin has been found to induce proliferation [15] and angiogenesis in human umbilical vein endothelial cells (HUVECs) *in vitro* [16]. Because osteogenesis and angiogenesis are the two important factors affecting bone fracture healing. Whether irisin can promote bone fracture healing is still unknown.

Previous studies on irisin were mainly consisted of epidemiological analyses of the irisin levels and fracture rates. Anastasilakis et al. found that the circulating irisin levels were lower in post-menopausal women with osteoporotic fractures [17]. Palermo et al. found an inverse correlation between the irisin levels and vertebral fragility fractures [18]. Yan et al. reported that low concentrations of irisin in older women were associated with an increased risk of hip fractures [19]. Finally, Serbest et al. found that irisin levels increased 60 days after a fracture stabilization operation, suggesting that it participates in the bone union process [20].

With the emerging findings that muscle may affect bone by acting as secretory endocrine organs besides exerting mechanical loading. Irisin act as the important monokine play key role in bone remodeling. As irisin is a monokine that can promote both osteogenesis and angiogenesis, it is important to determine its potential role in fracture healing. Here, we proposed an assumption that irisin can promote fracture healing through endochondral osteogenesis as well as angiogenesis. And we evaluated the role of irisin in fracture healing by using a model of closed mid-diaphyseal femur fractures with exogenous irisin treatment. The potential mechanisms underlying the effect of irisin on osteogenesis and angiogenesis were studied *in vitro*.

2. Methods

2.1. Animals

8- week-old male C57BL/6 mice with mature bone development [21] (*Mus musculus*) were purchased from Shanghai SIPPR BK Laboratory Animals Ltd (Shanghai, China). Mice were housed under a 12 h light/-dark cycle with free access to food and water. All animals used in this study have been ethically approved and received care in compliance with the institutional guidelines established by the Committee of Ethics on Animal Experiments at the Shanghai Jiao Tong University School of Medicine (Number: SH9H-202-A754-1).

2.2. Mouse femur fracture model and irisin treatment

Mouse femur fracture model was established to investigate the effects of irisin on fracture healing (M [22]. Briefly, mice were adequately anesthetized and analgesia to minimize suffering. The femurs were fractured in a controlled manner by scoring the bone and inducing a clean, transverse break with a beaver blade. Then, a closed mid-diaphyseal femur fracture model with stabilization was established by using a 23-gauge intramedullary needle (Yunaosi, Suzhou, China). After surgery, mice were randomly divided into control or irisin treatment group (N = 8 per group). A group (N = 8) per timepoint included 5 of them that underwent μCT scanning after microfil perfusion and the remaining 3 femurs were directly decalcified for sectioning. In addition, after 4 weeks (28 days), 7 animals per group underwent mechanical testing. Recombinant irisin (8880-IR-025; R&D, MN, USA) was administered intraperitoneally to mice at a dose of 100 μg/kg body weight every other day from the beginning on the first day after the surgery, which was proved that irisin have anabolic effect on bone [23,24]. The same volume of vehicle (0.9% normal saline) was used for the control group (Fig. 1A).

2.3. Radiography, fracture healing score and mechanical testing

After surgery, lateral radiograph of mice was taken for X-ray analysis by using the Faxitron MultiFocus system (50 kV; 200 mV; 32 ms; Tucson, AZ) for high-precision focus detection on 3, 7, 10, 15, 17 and 28 days post-fracture (DPF). All of radiographic images were individually quantified by three independent observers where Irisin and control samples were coded when the analysis was being performed. Fracture healing score (FHS) was assessed following three criteria: bone formation, bone union, and bone remodeling [25]. Every criterion was scored as either "0" which means "does not meet the criteria" or "1" which indicated that the criteria was met and is present by radiographic analysis. Right femurs of mice from the control and irisin groups on 28DPF were used for the three-point bending test (N = 7 mice per group). Intact femur containing callus after needle removal were wrapped in saline-soaked gauze and frozen at − 20 °C until use.

2.4. Histological evaluation

Right femurs of mice from the control and irisin groups were harvested 2, 3 and 4 weeks after the operation (N = 3 mice per group). Bone samples were immersed in 4% paraformaldehyde at 4 °C for 24 h, decalcified in 10% EDTA at 4 °C for 4 weeks, and finally embedded in paraffin. The femurs were sectioned (3 μm slices) along the longitudinal axis and stained with hematoxylin and eosin (H&E) and safranin O-fast green for histological analysis. Formaldehyde-fixed, paraffin-embedded bone tissue sections (5 μm) were assessed through immunohistochemical (IHC) staining. Sections were deparaffinized and hydrated with distilled water, followed by antigen recovery using 0.25% trypsin. Endogenous peroxidase activity was blocked by using peroxidase. Sections were incubated with primary antibodies against bone morphogenetic protein 2 (BMP2), vascular endothelial growth factor (VEGF), platelet endothelial

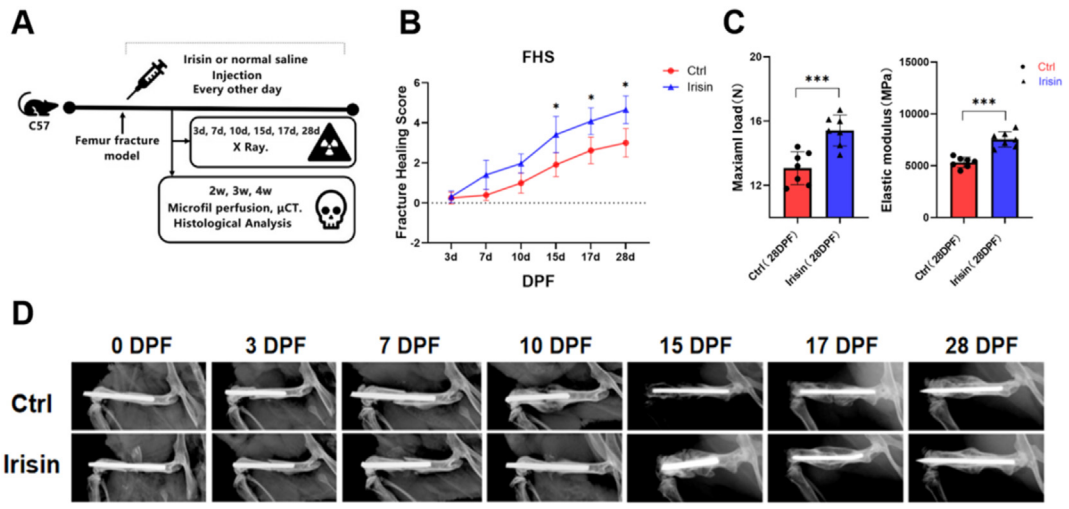

Fig. 1. Irisin treatment accelerates femur fracture healing in mice. (A) Design of the experiment. A mouse femur fracture model was established to investigate the effects of irisin on fracture healing. The fracture healing score (FHS), bone microstructure and formation of blood vessels were assessed at different time point (B) Evaluation of fracture healing using radiographs. FHS was assessed based on the following three criteria: bone formation, bone union, and bone remodeling, by observing the radiographs. *, $p < 0.05$ (C) Three-point bending testing of right femur at 28 days post-fracture (DPF) ($N = 7$ mice per group for femoral mechanical testing) (D) Representative X-ray images of the right femur at 0, 3, 7, 9, 15, 17 and 28 days post-fracture (DPF) ($N = 8$ mice per group for X-ray detection). Significance (P value) is calculated by two-way ANOVA analysis. *$P < 0.05$.

cell adhesion molecule-1 (CD31) (1:1,000, CST) overnight at 4 °C, followed by incubation with horseradish peroxidase-conjugated secondary antibodies. The peroxidase was reacted with 3,3′-diaminobenzidine (DAB), and the sections were then counterstained with Gill hematoxylin. A minimum of four samples were included in each group. After stained with H&E, bone fraction/Total callus (%) and cartilage fraction/Total callus (%) of the femurs were calculated by BIOQUANT OSTEO system (Bioquant; Nashville, TN, USA). While BMP2, CD31 and VEGF positive rate in the callus area were calculated by Image-Pro Plus software (Media Cybernetics; Rockville, MD, USA).

2.5. Microfil perfusion

Mice were euthanized with Microfil perfusion ($N = 5$ mice per group) (Flowtech, Carver, MA, USA). Briefly, the thoracic cavity is opened, an incision in the right atrial appendage is made as the outflow tract, and a vascular catheter is then penetrated the left ventricle. 20 mL (100 U/mL) of heparinized saline and 4% paraformaldehyde were sequentially perfused, followed by 10 mL of microfil at 2 mL/min. Finally, femurs were dissected at 4 °C overnight and continued to be decalcified for subsequent μCT scans.

Micro-computed tomography analysis of bone microstructure and angiogenesis.

Micro-computed tomography (μCT) scanning was performed to measure the microstructure of the bone callus ($N = 5$ mice per group). After euthanasia, the mouse femurs were dissected and fixed for 24 h in 10% PFA, transferred to 70% ethanol, and then prepared for μCT scanning using μCT80 (Scanco μCT80, SCANCO Medical AG, Brüttisellen, Switzerland), with an isotropic voxel size of 10 μm. The entire femur was scanned, and the volume of interest (VOI) used was 6 mm (600 slides), centered on the osteotomy line. Microarchitecture parameters were analyzed, including the bone volume fraction (BV/TV, %), connection density (Conn.Dens, 1/mm^3), trabecular number (Tb.N, 1/mm), trabecular thickness (Tb.Th, mm) and trabecular separation (Tb.Sp, mm). After evaluating the bone tissue, the femurs were placed in a decalcification solution at 4 °C for 4 weeks, and the solution was replaced every 48 h. Then the decalcified femurs were scanned again [26] to evaluate vessels in callus. Microarchitecture parameters were analyzed, including the vessel surface, vessel number, vessel volume fraction, and vessel surface/vessel volume (BS/BV, %).

2.6. Cell culture

HUVECs were purchased from the American Type Culture Collection (ATCC, Rockville, MD, USA). HUVECs were cultured in α-MEM (Gibco, Grand Island, NY, USA) supplemented with 10% fetal bovine serum (FBS, Gibco) at 37 °C in a humidified atmosphere with 5% CO_2.

Primary bone mesenchymal stem cells (bMSCs) were harvested from 4-week-old C57BL/6 male mice, as previously described [16]. Briefly, the femurs were collected on a super-clean bench, and the bone marrow cells were washed with Dulbecco's modified Eagle's medium (DMEM) and collected using a syringe. The bMSCs were cultured in DMEM (Gibco) supplemented with 10% FBS (Gibco), 50 U/mL penicillin, and 50 mg/mL streptomycin at 37 °C in a humidified atmosphere with 5% CO_2. After 24 h, non-adherent cells were removed by washing with phosphate-buffered saline (PBS), and third generation (designated "P3") primary bMSCs were used for the experiments. For osteogenic differentiation, cells were seeded in 6-well plates at a density of 1×10^6 cells/well. Osteogenesis was induced by adding osteogenic induction medium containing 10% FBS, 10 nM dexamethasone, 10 mM b-glycerophosphate, and 0.05 mM L-ascorbic acid-2-phosphate.

2.7. Cell migration assay

Cell migration assay was performed as previously described [27]. HUVECs were seeded on 6-well plates at a density of 1×10^6 cells/well. After growth to 85%–90% confluence, cells were scraped using a sterile disposable pipette tip to make a scratch wound. Then, the cells were washed twice with PBS and incubated in α-MEM with 2% FBS and 100 ng/mL irisin or the same volume of PBS [28]. After incubation for 12 h and 24 h, the wound area was photographed using an inverted phase contrast microscope (Olympus Corporation, Japan), and the relative percentage of wound healing was calculated using Image-Pro Plus software (Media Cybernetics; Rockville, MD, USA).

2.8. Tube formation assay

Tube formation assay was performed in Matrigel (BD Biosciences) according to the manufacturer's guidelines. HUVECs were suspended in DMEM with 2% FBS and 100 ng/mL irisin or the same volume of PBS. HUVECs (1.5×10^4) were seeded onto Matrigel-coated 96-well plates

and were incubated at 37 °C and 5% CO_2 for 6 h. The cells were then stained with a calcein-AM solution (Yeason, Shanghai, China) and 4′,6-diamidino-2-phenylindole. Tube formation was photographed using a fluorescence microscope (Olympus Corporation).

2.9. Alkaline phosphatase staining

After the induction of osteogenesis for 7 days with or without irisin (100 ng/mL) [24], bMSCs were fixed with 4% paraformaldehyde for 15 min and stained using an alkaline phosphatase (ALP) reagent kit (Nanjing Jiancheng Bioengineering Institute, China) according to the manufacturer's protocol. Cells were washed with PBS twice to remove the excess dye and then observed by inverted phase contrast microscope.

2.10. Alizarin red staining

After the induction of osteogenesis for 21 days with or without irisin (100 ng/mL), bMSCs were fixed with 4% paraformaldehyde for 15 min and stained with 0.1% alizarin red (Sigma–Aldrich) for 30 min at room temperature, according to the manufacturer's protocol. Cells were washed with PBS twice to remove the excess dye and then observed using an inverted phase contrast microscope.

2.11. RNA extraction and quantitative real-time PCR

Total RNA was purified from cells using TRIzol reagent (Invitrogen) according to the manufacturer's instructions. RNA concentration was assessed using a Nanodrop spectrophotometer (ND-1000; Thermo Scientific, USA). Equal amounts of RNA (1000 ng) were reversed-transcribed using a Bimake Supermix kit (Bimake). Diluted complementary DNA (cDNA) was subjected to quantitative real-time polymerase chain reaction (qRT-PCR, ABI 7500; Applied Biosystems, Foster City, CA, USA) using the SYBR Green reagent (Bimake), as described previously [29]. The qRT-PCR primers used in this study are listed in Table 1. Expression values were normalized to that of β-actin using the $2^{-\Delta\Delta Ct}$ method.

2.12. Statistical analysis

Data are presented as the mean ± standard deviation (SD). All *in vitro* data were obtained from three independent experiments. Differences between groups and different time point were analyzed by two-way ANOVA. Differences between two groups of *in vitro* results were analyzed by using Student's t test. Statistical analyses were performed using SPSS 24.0 software (SPSS Inc., Chicago, IL, USA) and GraphPad Prism 6 software. Statistical significance was set at $p < 0.05$.

Table 1
Primers used in realtime PCR.

Genes	Primer sequence
Mouse Osterix (OSX) 5′	CTCTCTGCTTGAGGAAGAAG
Mouse Osterix (OSX) 3′	GTCCATTGGTGCTTGAGAAG
Mouse Runx2 5′	CCGGGAATGATGAGAACTA
Mouse Runx2 3′	ACCGTCCACTGTCACTTT
Mouse OPG 5′	ACCCAGAAACTGGTCATCAGC
Mouse OPG 3′	CTGCAATACACACACTCATCACT
Mouse ALP 5′	GCCTGGATCTCATCAGTATTTGG
Mouse ALP 3′	GTTCAGTGCGGTTCCAGACAT
Mouse β-actin 3′	CACAGCCTGGATGGCTACGT
Human Ang1 5′	AGCGCCGAAGTCCAGAAAAC
Human Ang1 3′	TACTCTCACGACAGTTGCCAT
Human Ang2 5′	AACTTTCGGAAGAGCATGGAC
Human Ang2 3′	CGAGTCATCGTATTCGAGCGG
Human VEGFB 5′	GAGATGTCCCTGGAAGAACACA
Human VEGFB 3′	GAGTGGGATGGGTGATGTCAG
Human CD31/PECAM-1 5′	AACAGTGTTGACATGAAGAGCC
Human CD31/PECAM-1 3′	TGTAAAACAGCACGTCATCCTT
Human FGF2 5′	AGAAGAGCGACCCTCACATCA
Human FGF2 3′	CGGTTAGCACACACTCCTTTG
Human PDGF 5′	AGCACCTTCGTTCTGACCTG
Human PDGF 3′	TATTCTCCCGTGTCTAGCCCA
Human β-actin 5	CATGTACGTTGCTATCCAGGC
Human β-actin 3	CTCCTTAATGTCACGCACGAT

3. Results

3.1. Fracture healing score was increased after irisin injection

FHS showed that the irisin-treated group exhibited faster healing than control group according to the FHS at 7, 10, 15, 17 and 28 DPF ($p < 0.05$, Fig. 1B). Femurs of the irisin-treated and control group achieved union at 28DPF and the femurs were stronger in the irisin-treated group (Fig. 1C). After surgery, the fracture calluses were evaluated by using X-rays, which were taken at 0, 3, 7, 9, 15, 17 and 28 DPF (Fig. 1D).

3.2. Irisin increase bone microstructure and bone mineral density of fracture callus

Three-dimensional reconstruction of the femur fracture sites revealed callus formation at 2, 3 and 4 weeks post-surgery in both groups (Fig. 2A). BV/TV was significantly increased in the irisin-treated group at all time points, and Conn. Dens was only increased at 2 weeks post-surgery but did not differ at 3 and 4 weeks. Bone volume was increased in irisin-treated group at 3 weeks post-surgery than two weeks. The irisin-treated group gained more BMD after 2 weeks than the control group, indicating an accelerated mineralization after irisin treatment. Tb.N and Tb. Sp were reduced from 2 to 4 weeks. Compared to the control group, this downward trend was more pronounced in the irisin-treated group. While Tb.Th was the opposite of them, showing an upward trend in both groups at all time points (Fig. 2B). These parameters demonstrated better fracture healing in the irisin-treated group.

3.3. Irisin promote vascular ingrowth

After decalcification, the three-dimensional reconstruction of the fracture calluses revealed neovascularization in both groups at different time (Fig. 3A). The vessel surface and vessel volume fraction were significantly increased in the irisin-treated group at 3 weeks post-surgery than 2 weeks ($p < 0.05$), whereas the vessel number and BS/BV did not differ between the groups. However, moreangiogenesis at 2 and 3 weeks resulted in faster fracture healing by irisin and thus obviously less neovascularization in the irisin-treated group at 4 weeks (Fig. 3B).

3.4. Irisin increase osteogenesis and angiogenesis related protein expression

H&E staining revealed fracture callus formation in both groups during fracture healing (Fig. 4A). The infiltration of inflammatory cells in the early stage of fracture healing (2 weeks) was observed by H&E staining in both groups and infiltration had reduced and fibrocartilaginous callus formation was seen (Fig. 4A). Endochondral osteogenesis were observed and red-stained mucopolysaccharide showed better fibrocartilaginous callus formation (Fig. 4B). Bone fraction/Total callus (%) results shown that irisin promote mice bone formation during fracture healing and cartilage fraction was increased in the irisin-treated group (Fig. 4F), consistent with the Conn. Dens results. The expression of osteogenic factor, such as BMP2 (Fig. 4C, F), and angiogenic factors, such as CD31 (Fig. 4D, F), and VEGF (Fig. 4E and F) were higher in the irisin-treated group compared to the control group at weeks two and three. Because irisin-teatment accelerated fracture healing, all of the indicators were decreased significantly at 4 weeks (Fig. 4F).

3.5. Irisin increase osteogenesis of bMSCs

bMSCs were used to assess osteogenic induction; osteogenic differentiation was evidenced by ALP staining and alizarin red staining. ALP

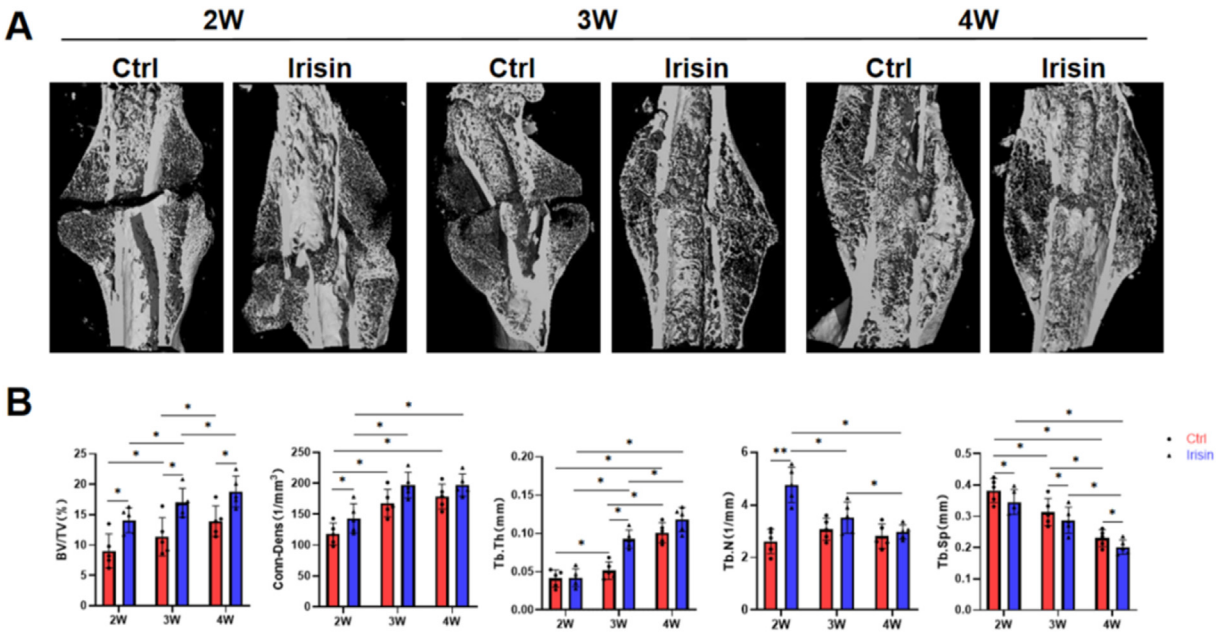

Fig. 2. Irisin treatment enhances the formation and mineralization of the fracture callus. (A)3D reconstruction of the femur fracture callus using μCT images at 2, 3 and 4 weeks. VOI was set 6 mm (600 slides), centered on the osteotomy line (B) Quantitation results of the bone volume (BV/TV) and connection density (Conn.Dens), trabecular number (Tb.N), trabecular thickness (Tb.Th) and trabecular separation (Tb.Sp) of the fracture callus. N = 5 mice per group. Significance (P value) is calculated by two-way ANOVA analysis. *P < 0.05.

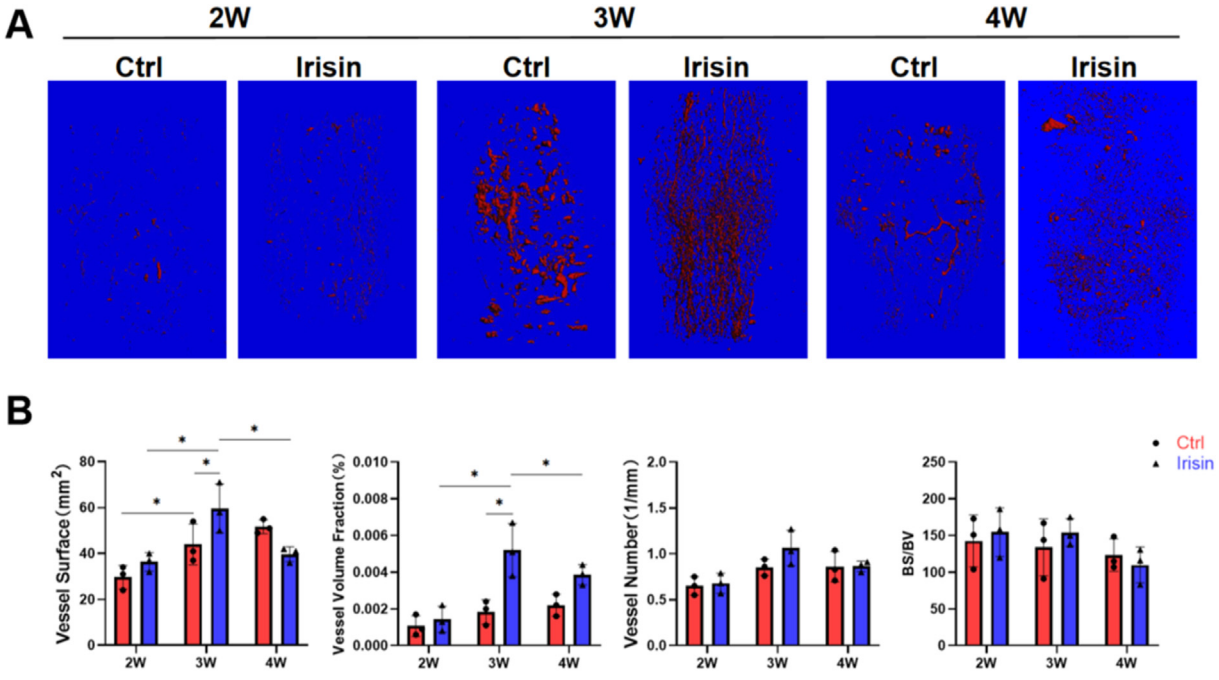

Fig. 3. Irisin treatment enhances the formation of blood vessels in the fracture callus. (A)3D reconstruction of the femur fracture callus using μCT images of angiograms, following Microfil perfusion at 2, 3 and 4 weeks. VOI was set 6 mm (600 slides), centered on the osteotomy line (B) Quantitation results of the vessel surface, vessel number, vessel volume fraction, and bone surface/bone volume fraction (BS/BV). N = 5 mice per group. Significance (P value) is calculated by two-way ANOVA analysis. *P < 0.05.

staining, an early marker of osteogenesis [30], was enhanced in the irisin-treated group on day 7 (Fig. 5A), and the measured OD value at 564 nm indicated that the irisin-treated group had more mineralized compartments than the control group during the late stage of osteogenesis (day 21, $p < 0.05$) (Fig. 5B). qRT-PCR analysis showed that the expression of osteogenic genes, such as *OPG*, *ALP*, *OCN*, and *BMP2*increased at all three time points (days 7, 14, and 21) in the irisin-treated group, whereas the expression of *OSX*, *Runx2* only increased on days 7 and 14 (Fig. 5C).

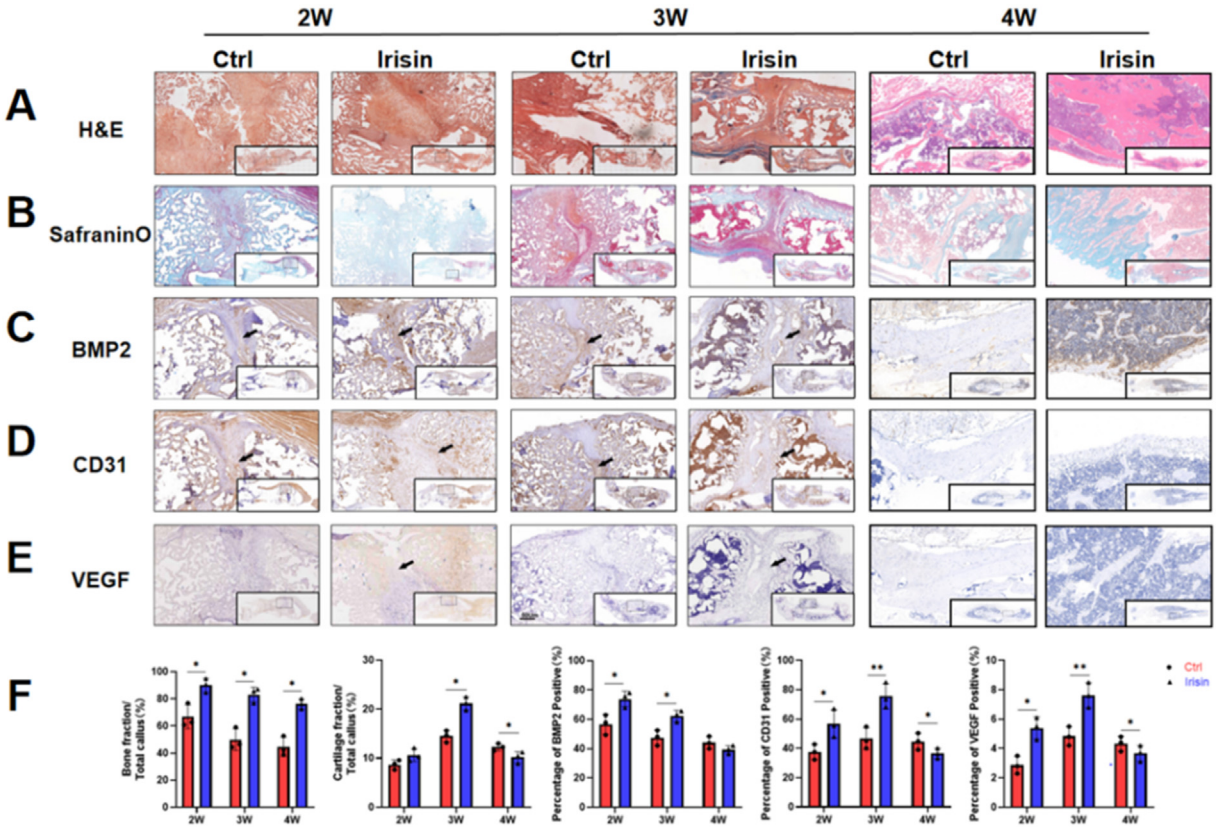

Fig. 4. Histological and immunohistochemical analyses of bone formation and angiogenesis in the fracture callus. (A) H&E results showed fracture callus formation was significantly increased after 2, 3 and 4 weeks in irisin group (B) Safranin O results showed cartilage fraction was increased in the irisin-treated group at week three (C) BMP2 (D) CD31, and (E) VEGF were higher in the irisin-treated group compared to the control group at weeks two and three. Black arrows: BMP2, CD31 or VEGF positive area in the fracture callus (F) Quantitation results of bone and cartilage fraction and BMP2, CD31 and VEGF positive area. N = 3. Significance (P value) is calculated by two-way ANOVA, *P < 0.05.

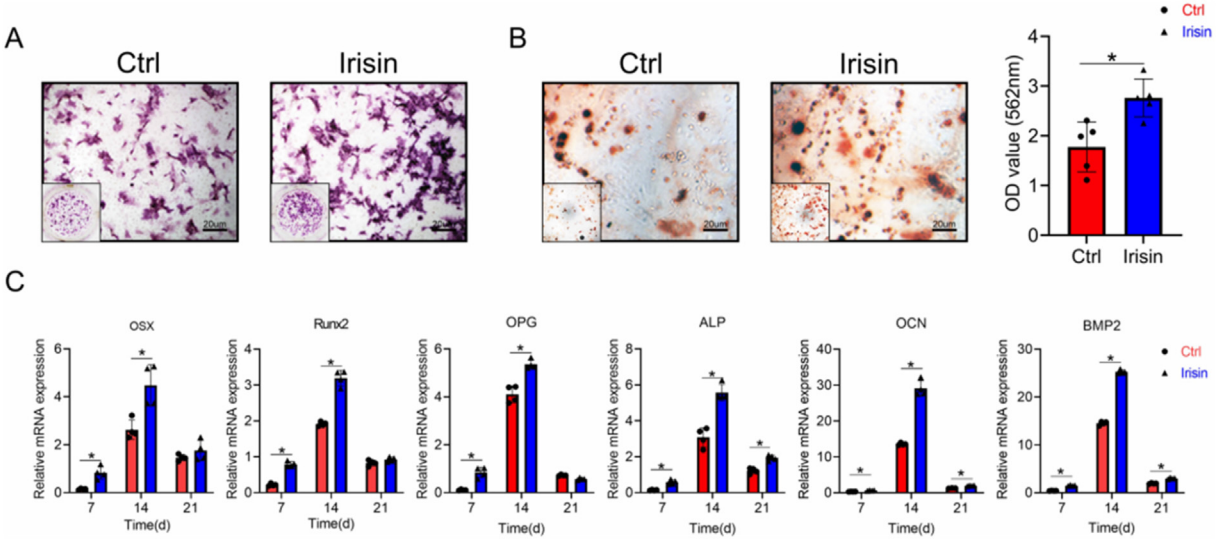

Fig. 5. Irisin promotes MSC osteogenesis. (A) ALP staining was enhanced in the irisin-treated group on day 7 after osteogenic induction for 7 days (B) The mineralization of bMSCs determined using alizarin red staining and quantitation after osteogenic induction for 21 days. OD value at 564 nm indicated that the irisin-treated group had more mineralized compartments than the control group (C) The osteogenic gene expression (*OSX*, *Runx2*, *OPG*, *ALP*, *OCN* and *BMP2*) of bMSCs were evaluated by using qRT-PCR. *OPG*, *ALP*, *OCN* and *BMP2*increased at all three time points (days 7, 14, and 21) in the irisin-treated group, whereas the expression of *OSX*, *Runx2* only increased on days 7 and 14. Significance (P value) is calculated by t-test, *P < 0.05.

3.6. Irisin increase angiogenesis of HUVECs

HUVECs were used to assess angiogenesis, and the effect of irisin on HUVEC migration was evaluated using a wound healing assay. Significantly more HUVECs migrated in the presence of irisin than in its absence (Fig. 6A). A tube-formation assay revealed that more vascular-like

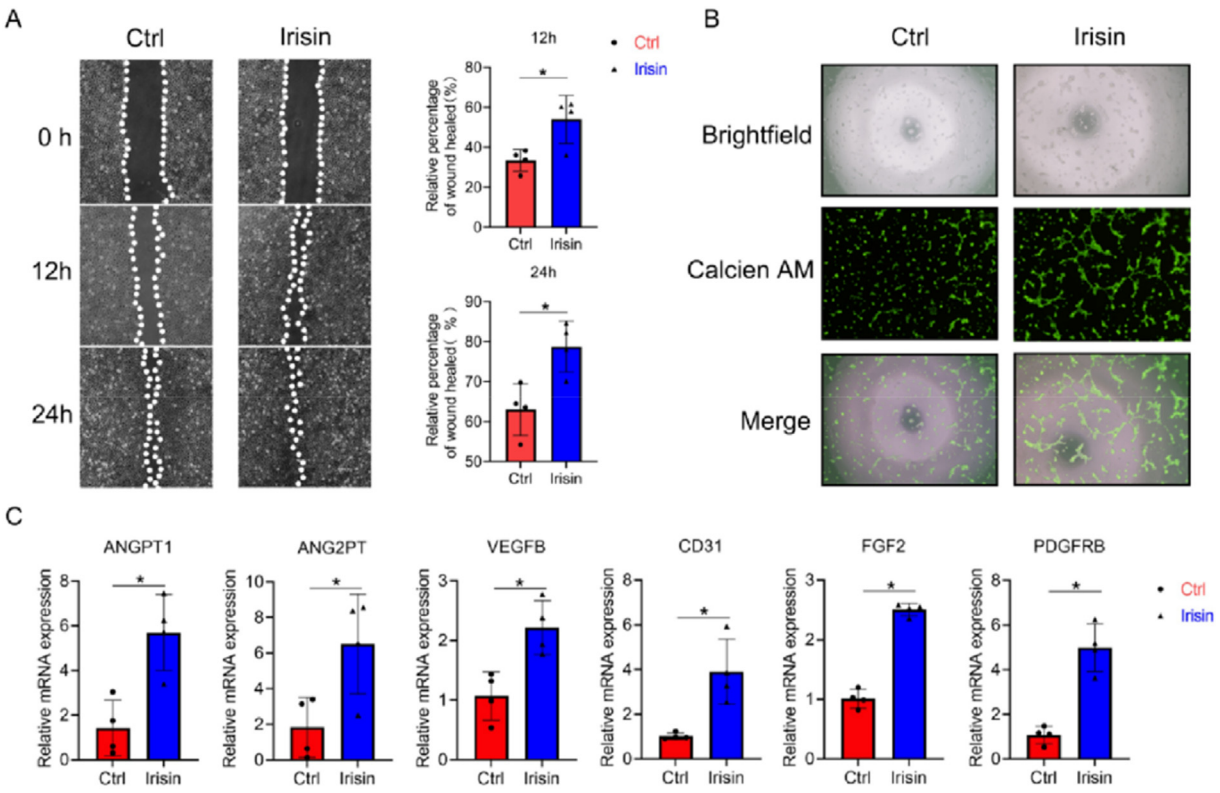

Fig. 6. Irisin promotes endothelial cell migration, tube formation, and angiogenetic gene expression. (A) HUVEC migration was evaluated using a cell migration assay, the dotted white lines showed the boundary of HUVECs, and the areas between them were calculated (B) Tube formation of HUVECs was assessed on solidified Matrigel and stained using calcein-AM, the merged image showed a clearer tube formation process (C) Angiogenetic gene expression (*ANG1*, *ANG2*, *VEGFb* and *CD31*, *FGF2*, and *PDGF*) in HUVECs, evaluated using qRT-PCR. Significance (P value) is calculated by t-test, *P $<$ 0.05.

structures were formed in the irisin-treated group in a dose-dependent manner (Fig. 6B). qRT-PCR analysis showed that the expression of *ANGT1, ANGPT2, VEGFB, FGF2, CD31 and PDGFRB* in the 200 ng/mL irisin-treated cells was higher than that in the control group at 24 h (Fig. 6C).

4. Discussion

The results of our study indicate that the callus size and volume, the degree of neovascularization after fracture increased after irisin treatment in mice. Moreover, the results of our *in vitro* study indicate that irisin enhances both osteogenesis and angiogenesis in cells. Our results suggest that irisin may accelerate fracture healing by promoting bone formation and angiogenesis.

Fracture healing is a complex and highly orchestrated biological process [31]. The muscles may act as endocrine organs during the fracture healing process, and myokines are considered important agents in this crosstalk. Based on clinical research, several agents play similar roles in fracture healing. BMP2 was approved by the FDA as an osteoinductive factor in fracture treatment [32]. However, following the wide application of BMP2, an increasing number of studies have demonstrated its clinical side effects, including ectopic bone reconstruction, osteoclast-induced bone resorption, bone cyst formation, and inflammatory complications [33,34].

Angiogenesis is a critical process in fracture healing [35,36]. Further, in diseases such as diabetes, an impaired blood vessel function can interfere with this process. Angiogenic factors, including VEGF, BMPs, FGF-1, and TGF-β, represent another class of proteins that drive fracture repair by mediating the invasion of the soft callus through endothelial cells [2]. The inhibition of VEGF activity impaired femoral fracture healing in mice [37]. Our results indicated that irisin can increase bone mineralization. Furthermore, our results showed that bone volume was significantly increased in the irisin-treated group at both time points, while the vessel surface and vessel volume fraction were significantly increased in the irisin-treated group after 3 weeks treatment, but had no difference after 2- and 4-weeks treatment. Diane P Hu et al. [38]found the vasculature coordinates chondrocyte to osteoblast transdifferentiation. We hypothesized that irisin can increase bone mineralization through osteoblasts on the one hand, on the other hand, irisin can promote vascular ingrowth which might promote chondrocyte to osteoblast transformation during bone fracture healing.

In our study, the formation and mineralization of the fracture callus occurred faster in the irisin-treated group than in the control group, and our *in vitro* studies indicated that irisin enhanced osteogenesis in bMSCs by improving proliferation and mineralization. Further, the mRNA expression of *OCN* and *Runx2* was enhanced by irisin. Runx2 is a critical transcription factor involved in the development and differentiation of osteoblasts [39], and can upregulate levels of bone sialoprotein and osteocalcin, which are two major components of bone extracellular matrix synthesized exclusively by osteoblastic cells [40]. Runx2 also has an important role in the repair of bone tissue (Z. C [41]. Xu et al. found high expression levels of relevant osteogenic genes, including *Runx2* and *OCN*, in irisin-treated (1 mmol/L) osteoporosis SD rat bone tissues [42]. Colaianni et al. found that irisin treatment (100 μg/kg) attenuated the OPG decrease in unloading mice [14] and that irisin from conditioned media collected from the myoblasts of exercised mice induced osteoblast differentiation *in vitro* (G [13]. Qiao et al. found that both r-irisin and irisin-containing conditioned medium promoted the proliferation, differentiation, and mineralization of MC3T3-E1 cells and primary osteoblasts through the activities of Runx2, OSX, ALP, Col-1, OCN, and OPN [43].

After fracture, hematoma formation allows the blood vessel formation around the fracture site. Cells in the fracture callus depend on angiogenesis for oxygen and nutrient delivery. During fracture healing,

angiogenesis induced vessels appear during the stage of fibrocartilaginous callus formation. Vessels form in the fracture callus and induce bone formation. When angiogenesis is impaired, the fracture healing process is impacted (Y [44]. The unique process of angiogenesis has an important effect on mineralization and morphology in the bone repair process [45]. Moreover, osteoblast precursors, but not mature osteoblasts, travel to fractured bone areas [46]. A series of cytokines are involved in this process, including VEGF (Z. [47], FGF [40]. VEGF promotes angiogenesis and increases bone formation via the ingress of osteoblast progenitor cells and is expressed in the fracture callus during the early stage. CD31 is related to angiogenesis and improves vessel formation under ischemic conditions after *in vivo* transplantation; CD31+ cell transplantation can promote the fracture healing process [48]. In our study, we found that the surface and volume fraction of vessels increased in the callus in the irisin-treated group at 3 weeks after fracture and that the expression of CD31 and VEGF increased in the callus area. This indicates that angiogenesis, paired with accelerated callus formation and mineralization processes, promotes fracture healing. In addition, we found that irisin promoted the angiogenesis of HUVECs in terms of both migration and tube formation, consistent with previous *in vitro* studies [15,16]. HUVECs are a useful tool to investigate the process of angiogenesis in the bone fracture callus [49] and in other diseases and conditions, including diabetes and myocardial infarction. Deng et al. found that irisin alleviated the inflammation induced by advanced glycation end products in HUVECs [50]. Song et al. found that irisin can promote HUVEC proliferation and angiogenesis through the Erk signaling pathway [15,16]. Liao et al. confirmed the phosphorylation of ERK in HUVECs and the migration and wound-healing effects induced by irisin [51]. Rana et al. found that irisin can increase the expression of E-selectin [52], which is associated with tumor angiogenesis [53].

On the one hand, previous studies have indicated that irisin can activate MAPK signaling pathways, including the Erk signaling pathway, in osteoblasts, MSCs, and HUVECs. On the other hand, the expression and activation of angiogenic factors can be regulated by MAPK signaling pathways, including Runx2 phosphorylation [54] and expression of receptor tyrosine kinases, such as PDGF [55,56]. Therefore, drugs that affect both angiogenesis and osteogenesis will help improve fracture healing by accelerating the formation and mineralization of the callus [57]. Furthermore, irisin may promote Fractur healing through increased mechanical loading from skeletal muscle. Reza et al. [58] found irisin could enhance grip strength of uninjured mice muscle by improving regeneration and induces hypertrophy.

Our study has some limitations. First, we did not measure the serum irisin levels in mice after irisin treatment, which would demonstrate the effectiveness of systemic drug delivery. However, other studies have shown that intraperitoneal administration has a strong regulatory effect on bone tissues in mice [14,59]. Second, our investigation of cell signaling pathways was limited; although the osteogenesis and angiogenesis results of the *in vitro* experiments were consistent with the findings of our *in vivo* fracture model, the internal regulatory mechanisms underlying the effects of irisin still need to be clarified.

In conclusion, the findings of this study indicate that irisin can aid in the formation of the bone callus and promote the fracture healing process. However, the detailed mechanisms underlying the mode of action of irisin remain unclear, and more studies are needed. Since Kim H. et al. [60]. Found irisin mediates effects on bone and fat via αV integrin receptors, and Teklemariam T et al. [61] showed that HUVEC express αv, αvβ3, αvβ5, α6, β1, and β3 integrin receptors. Irisin may affect bone cells and HUEC via αv integrin receptors. Future research should confirm the signaling pathway that irisin affect HUVEC, which will help to understand the mechanism of muscle affect bone fracture healing.

Author contributions

ZH, JD, and ZY were involved in the design of the study, basic analysis of data, drafting of manuscript, and revising it for critical knowledge content. ZH and JD performed the statistical analysis. JC, XH, DT, HL, and MY were involved in the acquisition of data, drafting of manuscript, and revising it critically for critical knowledge content. All authors have read and approved the final submitted manuscript.

Data availability statement

Embargo on data because of commercial restrictions.

Declaration of competing interest

The content is solely the responsibility of the authors. The funding body was not involved in the design, collection, analysis, and interpretation of data, or the writing of the manuscript. The authors declare that they have no conflicts of interest or financial ties to disclose.

Acknowledgements

This work was supported by grants from the National Natural Science Foundation of China (No. 12172223, 11872251) and Shanghai Science and Technology Committee (grant no. 19140900104).

References

[1] Santolini E, West R, Giannoudis PV. Risk factors for long bone fracture non-union: a stratification approach based on the level of the existing scientific evidence. Injury 2015;46(Suppl 8):S8–s19. https://doi.org/10.1016/s0020-1383(15)30049-8.
[2] Schindeler A, McDonald MM, Bokko P, Little DG. Bone remodeling during fracture repair: the cellular picture. Semin Cell Dev Biol 2008;19(5):459–66. https://doi.org/10.1016/j.semcdb.2008.07.004.
[3] Ding ZC, Lin YK, Gan YK, Tang TT. Molecular pathogenesis of fracture nonunion. J Orthop Translat 2018;14:45–56. https://doi.org/10.1016/j.jot.2018.05.002.
[4] Einhorn TA, Gerstenfeld LC. Fracture healing: mechanisms and interventions. Nat Rev Rheumatol 2015;11(1):45–54. https://doi.org/10.1038/nrrheum.2014.164.
[5] Wang T, Zhang X, Bikle DD. Osteogenic differentiation of periosteal cells during fracture healing. J Cell Physiol 2017;232(5):913–21. https://doi.org/10.1002/jcp.25641.
[6] Gustilo RB, Mendoza RM, Williams DN. Problems in the management of type III (severe) open fractures: a new classification of type III open fractures. J Trauma 1984;24(8):742–6. https://doi.org/10.1097/00005373-198408000-00009.
[7] Davis KM, Griffin KS, Chu TG, Wenke JC, Corona BT, McKinley TO, et al. Muscle-bone interactions during fracture healing. J Musculoskelet Neuronal Interact 2015;15(1):1–9. https://pubmed.ncbi.nlm.nih.gov/25730647. https://www.ncbi.nlm.nih.gov/pmc/articles/PMC4433554/. Retrieved from.
[8] Chan JK, Harry L, Williams G, Nanchahal J. Soft-tissue reconstruction of open fractures of the lower limb: muscle versus fasciocutaneous flaps. Plast Reconstr Surg 2012;130(2):284e–95e. https://doi.org/10.1097/PRS.0b013e3182589e63.
[9] Kai MC, Anderson M, Lau EM. Exercise interventions: defusing the world's osteoporosis time bomb. Bull World Health Organ 2003;81(11):827–30.
[10] Wang Z, Bian L, Mo C, Shen H, Zhao LJ, Su K-J, et al. Quantification of aminobutyric acids and their clinical applications as biomarkers for osteoporosis. Commun Biol 2020;3(1):39. https://doi.org/10.1038/s42003-020-0766-y.
[11] Erickson HP. Irisin and FNDC5 in retrospect: an exercise hormone or a transmembrane receptor? Adipocyte 2013;2(4):289–93. https://doi.org/10.4161/adip.26082.
[12] Bostrom P, Wu J, Jedrychowski MP, Korde A, Ye L, Lo JC, et al. A PGC1-alpha-dependent monokine that drives brown-fat-like development of white fat and thermogenesis. Nature 2012;481(7382):463–8. https://doi.org/10.1038/nature10777.
[13] Colaianni G, Cuscito C, Mongelli T, Oranger A, Mori G, Brunetti G, et al. Irisin enhances osteoblast differentiation in vitro. Internet J Endocrinol 2014:902186. https://doi.org/10.1155/2014/902186. 2014.
[14] Colaianni G, Mongelli T, Cuscito C, Pignataro P, Lippo L, Spiro G, et al. Irisin prevents and restores bone loss and muscle atrophy in hind-limb suspended mice. Sci Rep 2017;7(1):2811. https://doi.org/10.1038/s41598-017-02557-8. 2811.
[15] Song H, Wu F, Zhang Y, Zhang Y, Wang F, Jiang M, et al. Irisin promotes human umbilical vein endothelial cell proliferation through the ERK signaling pathway and partly suppresses high glucose-induced apoptosis. PLoS One 2014;9(10):e110273. https://doi.org/10.1371/journal.pone.0110273. e110273.
[16] Wu F, Song H, Zhang Y, Zhang Y, Mu Q, Jiang M, et al. Irisin induces angiogenesis in human umbilical vein endothelial cells in vitro and in zebrafish embryos in vivo via activation of the ERK signaling pathway. PLoS One 2015;10(8):e0134662. https://doi.org/10.1371/journal.pone.0134662. e0134662.
[17] Anastasilakis AD, Polyzos SA, Makras P, Gkiomisi A, Bisbinas I, Katsarou A, et al. Circulating irisin is associated with osteoporotic fractures in postmenopausal women with low bone mass but is not affected by either teriparatide or denosumab treatment for 3 months. Osteoporos Int 2014;25(5):1633–42. https://doi.org/10.1007/s00198-014-2673-x.

[18] Palermo A, Strollo R, Maddaloni E, Tuccinardi D, D'Onofrio L, Briganti SI, et al. Irisin is associated with osteoporotic fractures independently of bone mineral density, body composition or daily physical activity. Clin Endocrinol 2015;82(4):615–9. https://doi.org/10.1111/cen.12672.
[19] Yan J, Liu HJ, Guo WC, Yang J. Low serum concentrations of Irisin are associated with increased risk of hip fracture in Chinese older women. Joint Bone Spine 2018;85(3):353–8. https://doi.org/10.1016/j.jbspin.2017.03.011.
[20] Serbest S, Tiftikci U, Tosun HB, Kisa U. The irisin hormone profile and expression in human bone tissue in the bone healing process in patients. Med Sci Monit 2017;23:4278–83. https://doi.org/10.12659/msm.906293.
[21] Ferguson VL, Ayers RA, Bateman TA, Simske SJ. Bone development and age-related bone loss in male C57BL/6J mice. Bone 2003;33(3):387–98. https://doi.org/10.1016/s8756-3282(03)00199-6.
[22] Zhang M, Ho H-c, Sheu T-j, Breyer MD, Flick LM, Jonason JH, et al. EP1(-/-) mice have enhanced osteoblast differentiation and accelerated fracture repair. J Bone Miner Res 2011;26(4):792–802. https://doi.org/10.1002/jbmr.272.
[23] Colaianni G, Cuscito C, Mongelli T, Pignataro P, Buccoliero C, Liu P, et al. The monokine irisin increases cortical bone mass. Proc Natl Acad Sci USA 2015;112(39):12157. https://doi.org/10.1073/pnas.1516622112.
[24] He Z, Li H, Han X, Zhou F, Du J, Yang Y, et al. Irisin inhibits osteocyte apoptosis by activating the Erk signaling pathway in vitro and attenuates ALCT-induced osteoarthritis in mice. Bone 2020;141:115573. https://doi.org/10.1016/j.bone.2020.115573.
[25] Yuasa M, Saito M, Molina C, Moore-Lotridge SN, Benvenuti MA, Mignemi NA, et al. Unexpected timely fracture union in matrix metalloproteinase 9 deficient mice. PLoS One 2018;13(5):e0198088. https://doi.org/10.1371/journal.pone.0198088.
[26] Suen PK, He Y-X, Chow DHK, Huang L, Li C, Ke HZ, et al. Sclerostin monoclonal antibody enhanced bone fracture healing in an open osteotomy model in rats. J Orthop Res 2014;32(8):997–1005. https://doi.org/10.1002/jor.22636.
[27] Zheng H, Yu Z, Deng M, Cai Y, Wang X, Xu Y, et al. Fat extract improves fat graft survival via proangiogenic, anti-apoptotic and pro-proliferative activities. Stem Cell Res Ther 2019;10(1):174. https://doi.org/10.1186/s13287-019-1290-1.
[28] Lu J, Xiang G, Liu M, Mei W, Xiang L, Dong J. Irisin protects against endothelial injury and ameliorates atherosclerosis in apolipoprotein E-Null diabetic mice. Atherosclerosis 2015;243(2):438–48.
[29] Zhou F, Mei J, Yang S, Han X, Li H, Yu Z, et al. Modified ZIF-8 nanoparticles attenuate osteoarthritis by reprogramming the metabolic pathway of synovial macrophages. ACS Appl Mater Interfaces 2020;12(2):2009–22. https://doi.org/10.1021/acsami.9b16327.
[30] Tsai MT, Li WJ, Tuan RS, Chang WH. Modulation of osteogenesis in human mesenchymal stem cells by specific pulsed electromagnetic field stimulation. J Orthop Res 2009;27(9):1169–74. https://doi.org/10.1002/jor.20862.
[31] Harwood PJ, Newman JB, Michael ALR. (ii) an update on fracture healing and non-union. Orthop Traumatol 2010;24(1):9–23. https://doi.org/10.1016/j.mporth.2009.12.004.
[32] Urist MR. Bone: formation by autoinduction. Science 1965;150(3698):893–9. https://doi.org/10.1126/science.150.3698.893.
[33] James AW, LaChaud G, Shen J, Asatrian G, Nguyen V, Zhang X, et al. A review of the clinical side effects of bone morphogenetic protein-2. Tissue Eng B Rev 2016;22(4):284–97. https://doi.org/10.1089/ten.TEB.2015.0357.
[34] Xie K, Wang L, Guo Y, Zhao S, Yang Y, Dong D, et al. Effectiveness and safety of biodegradable Mg-Nd-Zn-Zr alloy screws for the treatment of medial malleolar fractures. J Orthop Translat 2021;27:96–100. https://doi.org/10.1016/j.jot.2020.11.007.
[35] Ali S, Singh A, Mahdi AA, Srivastava RN. CYR61-An angiogenic biomarker to early predict the impaired healing in diaphyseal tibial fractures. J Orthop Translat 2017;10:5–11. https://doi.org/10.1016/j.jot.2017.02.004.
[36] Fang TD, Salim A, Xia W, Nacamuli RP, Guccione S, Song HM, et al. Angiogenesis is required for successful bone induction during distraction osteogenesis. J Bone Miner Res 2005;20(7):1114–24. https://doi.org/10.1359/jbmr.050301.
[37] Street J, Bao M, deGuzman L, Bunting S, Peale Jr FV, Ferrara N, et al. Vascular endothelial growth factor stimulates bone repair by promoting angiogenesis and bone turnover. Proc Natl Acad Sci U S A 2002;99(15):9656–61. https://doi.org/10.1073/pnas.152324099.
[38] Hu DP, Ferro F, Yang F, Taylor AJ, Chang W, Miclau T, et al. Cartilage to bone transformation during fracture healing is coordinated by the invading vasculature and induction of the core pluripotency genes. Development 2017;144(2):221–34. https://doi.org/10.1242/dev.130807.
[39] Zhu J, Liu Y, Chen C, Chen H, Huang J, Luo Y, et al. Cyasterone accelerates fracture healing by promoting MSCs migration and osteogenesis. J Orthop Translat 2021;28:28–38. https://doi.org/10.1016/j.jot.2020.11.004.
[40] Kennedy OD, Laudier DM, Majeska RJ, Sun HB, Schaffler MB. Osteocyte apoptosis is required for production of osteoclastogenic signals following bone fatigue in vivo. Bone 2014;64C:132–7. S8756-3282(14)00123-9 [pii], 10.1016/j.bone.2014.03.049.
[41] Liu ZC, Xu YL, Jiang Y, Liu Y, Wei ZC, Liu SG, et al. Low-expression of lncRNA-ANCR promotes tibial fracture healing via targeting RUNX2. Eur Rev Med Pharmacol Sci 2019;23(3 Suppl):60–6. https://doi.org/10.26355/eurrev_201908_18629.
[42] Xu L, Shen L, Yu X, Li P, Wang Q, Li C. Effects of irisin on osteoblast apoptosis and osteoporosis in postmenopausal osteoporosis rats through upregulating Nrf2 and inhibiting NLRP3 inflammasome. Exp Ther Med 2020;19(2):1084–90.
[43] Qiao X, Nie Y, Ma Y, Chen Y, Cheng R, Yin W, et al. Irisin promotes osteoblast proliferation and differentiation via activating the MAP kinase signaling pathways. Sci Rep 2016;6:18732. https://doi.org/10.1038/srep18732.
[44] Liu Y, Fang J, Zhang Q, Zhang X, Cao Y, Chen W, et al. Wnt10b-overexpressing umbilical cord mesenchymal stem cells promote critical size rat calvarial defect healing by enhanced osteogenesis and VEGF-mediated angiogenesis. J Orthop Translat 2020;23:29–37. https://doi.org/10.1016/j.jot.2020.02.009.
[45] Ben Shoham A, Rot C, Stern T, Krief S, Akiva A, Dadosh T, et al. Deposition of collagen type I onto skeletal endothelium reveals a new role for blood vessels in regulating bone morphology. Development 2016;143(21):3933–43. https://doi.org/10.1242/dev.139253.
[46] Maes C, Kobayashi T, Selig MK, Torrekens S, Roth SI, Mackem S, et al. Osteoblast precursors, but not mature osteoblasts, move into developing and fractured bones along with invading blood vessels. Dev Cell 2010;19(2):329–44. https://doi.org/10.1016/j.devcel.2010.07.010.
[47] Zhang Z, Zhang Y, Zhou Z, Shi H, Qiu X, Xiong J, et al. BDNF regulates the expression and secretion of VEGF from osteoblasts via the TrkB/ERK1/2 signaling pathway during fracture healing. Mol Med Rep 2017;15(3):1362–7. https://doi.org/10.3892/mmr.2017.6110.
[48] Sass FA, Schmidt-Bleek K, Ellinghaus A, Filter S, Rose A, Preininger B, et al. CD31+ cells from peripheral blood facilitate bone regeneration in biologically impaired conditions through combined effects on immunomodulation and angiogenesis. J Bone Miner Res 2017;32(5):902–12. https://doi.org/10.1002/jbmr.3062.
[49] Levy S, Feduska JM, Sawant A, Gilbert SR, Hensel JA, Ponnazhagan S. Immature myeloid cells are critical for enhancing bone fracture healing through angiogenic cascade. Bone 2016;93:113–24. https://doi.org/10.1016/j.bone.2016.09.018.
[50] Deng X, Huang W, Peng J, Zhu TT, Sun XL, Zhou XY, et al. Irisin alleviates advanced glycation end products-induced inflammation and endothelial dysfunction via inhibiting ROS-NLRP3 inflammasome signaling. Inflammation 2018;41(1):260–75. https://doi.org/10.1007/s10753-017-0685-3.
[51] Liao Q, Qu S, Tang LX, Li LP, He DF, Zeng CY, et al. Irisin exerts a therapeutic effect against myocardial infarction via promoting angiogenesis. Acta Pharmacol Sin 2019;40(10):1314–21. https://doi.org/10.1038/s41401-019-0230-z.
[52] Rana KS, Pararasa C, Afzal I, Nagel DA, Hill EJ, Bailey CJ, et al. Plasma irisin is elevated in type 2 diabetes and is associated with increased E-selectin levels. Cardiovasc Diabetol 2017;16(1):147. https://doi.org/10.1186/s12933-017-0627-2. 147.
[53] Borentain P, Carmona S, Mathieu S, Jouve E, El-Battari A, Gérolami R. Inhibition of E-selectin expression on the surface of endothelial cells inhibits hepatocellular carcinoma growth by preventing tumor angiogenesis. Cancer Chemother Pharmacol 2016;77(4):847–56. https://doi.org/10.1007/s00280-016-3006-x.
[54] Chevallier N, Anagnostou F, Zilber S, Bodivit G, Maurin S, Barrault A, et al. Osteoblastic differentiation of human mesenchymal stem cells with platelet lysate. Biomaterials 2010;31(2):270–8. https://doi.org/10.1016/j.biomaterials.2009.09.043.
[55] Rieg AD, Suleiman S, Anker C, Verjans E, Rossaint R, Uhlig S, et al. PDGF-BB regulates the pulmonary vascular tone: impact of prostaglandins, calcium, MAPK- and PI3K/AKT/mTOR signalling and actin polymerisation in pulmonary veins of Guinea pigs. Respir Res 2018;19(1):120. https://doi.org/10.1186/s12931-018-0829-5.
[56] Sun X, Li X, Qi H, Hou X, Zhao J, Yuan X, et al. MiR-21 nanocapsules promote early bone repair of osteoporotic fractures by stimulating the osteogenic differentiation of bone marrow mesenchymal stem cells. J Orthop Translat 2020;24:76–87. https://doi.org/10.1016/j.jot.2020.04.007.
[57] Lim JC, Ko KI, Mattos M, Fang M, Zhang C, Feinberg D, et al. TNFα contributes to diabetes impaired angiogenesis in fracture healing. Bone 2017;99:26–38. https://doi.org/10.1016/j.bone.2017.02.014.
[58] Reza MM, Subramaniyam N, Sim CM, Ge X, Sathiakumar D, McFarlane C, et al. Irisin is a pro-myogenic factor that induces skeletal muscle hypertrophy and rescues denervation-induced atrophy. Nat Commun 2017;8(1):1104. https://doi.org/10.1038/s41467-017-01131-0.
[59] Storlino G, Colaianni G, Sanesi L, Lippo L, Brunetti G, Errede M, et al. Irisin prevents disuse-induced osteocyte apoptosis. J Bone Miner Res 2020;35(4):766–75. https://doi.org/10.1002/jbmr.3944.
[60] Kim H, Wrann CD, Jedrychowski M, Vidoni S, Kitase Y, Nagano K, et al. Irisin mediates effects on bone and fat via alphaV integrin receptors. Cell 2018;175(7):1756–1768 e1717. https://doi.org/10.1016/j.cell.2018.10.025.
[61] Teklemariam T, Seoane AI, Ramos CJ, Sanchez EE, Lucena SE, Perez JC, et al. Functional analysis of a recombinant PIII-SVMP, GST-acocostatin; an apoptotic inducer of HUVEC and HeLa, but not SK-Mel-28 cells. Toxicon 2011;57(5):646–56. https://doi.org/10.1016/j.toxicon.2011.01.007.